Simulating Dynamic Quantum Phase Transitions in Photonic Quantum Walks

Kunkun Wang,[1,2] Xingze Qiu,[3,4] Lei Xiao,[1,2] Xiang Zhan,[1,2] Zhihao Bian,[1,2] Wei Yi,[3,4,*] and Peng Xue[1,2,5,†]
[1]*Beijing Computational Science Research Center, Beijing 100084, China*
[2]*Department of Physics, Southeast University, Nanjing 211189, China*
[3]*Key Laboratory of Quantum Information, University of Science and Technology of China, CAS, Hefei 230026, China*
[4]*Synergetic Innovation Center in Quantum Information and Quantum Physics, University of Science and Technology of China, CAS, Hefei 230026, China*
[5]*State Key Laboratory of Precision Spectroscopy, East China Normal University, Shanghai 200062, China*

(Received 3 July 2018; revised manuscript received 2 November 2018; published 16 January 2019)

Signaled by nonanalyticities in the time evolution of physical observables, dynamic quantum phase transitions (DQPTs) emerge in quench dynamics of topological systems and possess an interesting geometric origin captured by dynamic topological order parameters (DTOPs). In this Letter, we report the experimental study of DQPTs using discrete-time quantum walks of single photons. We simulate quench dynamics between distinct Floquet topological phases using quantum-walk dynamics and experimentally characterize DQPTs and the underlying DTOPs through interference-based measurements. The versatile photonic quantum-walk platform further allows us to experimentally investigate DQPTs for mixed states and in parity-time-symmetric nonunitary dynamics for the first time. Our experiment directly confirms the relation between DQPTs and DTOPs in quench dynamics of topological systems and opens up the avenue of simulating emergent topological phenomena using discrete-time quantum-walk dynamics.

DOI: 10.1103/PhysRevLett.122.020501

The study of phase transitions lies at the core of the description of equilibrium states of matter [1]. Besides conventional continuous phase transitions that are signaled by symmetry breaking, topological phase transitions, characterized by the change of topology in their ground-state wave functions, have attracted much attention since the discovery of quantum Hall effects [2,3]. Recent experimental progress has further led to the exciting possibility of creating novel quantum phases of matter in dynamic processes [4–19] and thus raised the challenging question on the understanding of emergent phases and phase transitions in nonequilibrium dynamics.

Proposed as temporal analogs to continuous phase transitions, dynamic quantum phase transitions (DQPTs) are associated with nonanalyticities in the time evolution of physical observables [20–22] and have been experimentally observed recently [15–18]. For continuous phase transitions in equilibrium systems, the free energy becomes nonanalytic at critical points, associated with complex-partition-function zeros known as Fisher [23] or Lee-Yang zeros [24,25]. Analogously, DQPT occurs as a consequence of the emergence of dynamic Fisher zeros, where the Loschmidt amplitude $G(t) = \langle\psi(0)|\psi(t)\rangle$ [26], the analog of the partition function, vanishes at critical times. This leads to nonanalyticities in the rate function $g(t) = -1/N \ln|G(t)|^2$, which serves as the dynamic free energy [22]. Here $|\psi(t)\rangle$ is the time-evolved state, and N is the overall degrees of freedom of the system. Whereas it is still unclear to what extent key concepts of continuous phase transitions can be extended to describe DQPTs, an intriguing discovery is the geometric origin of DQPTs, captured by dynamic topological order parameters (DTOPs), which suggests the intimate connection between DQPTs and emergent topological phenomena in dynamic processes [27–31].

A relevant dynamic process here is the quench of topological systems, where the ground state $|\psi^i\rangle$ of the initial Hamiltonian H^i evolves under the final Hamiltonian H^f. Here two different types of dynamic phase transition can occur: topological DQPTs, whose occurrence is intimately related to the topology of H^i and H^f, and accidental DQPTs, which are to the contrary. Specifically, for quench dynamics of one-dimensional topological systems, topological DQPTs necessarily exist when ground states of H^i and H^f belong with distinct topological phases [32–34]. These topological DQPTs provide a crucial link between static topological phases and dynamic topological phenomena. In two dimensions, topological DQPTs recently observed in cold atomic gases are accompanied by dynamic vortices [8], which serve as the effective order parameter. In one dimension, on the other hand, relations between DQPTs and DTOPs have yet to be experimentally investigated.

In this Letter, we report the experimental simulation of topological DQPTs using discrete-time quantum walks (QWs) [35–39] of single photons in one dimension. We map single-photon QWs to many-body quench dynamics between Floquet topological phases of fermions, where topological DQPTs naturally emerge. Specifically, we probe

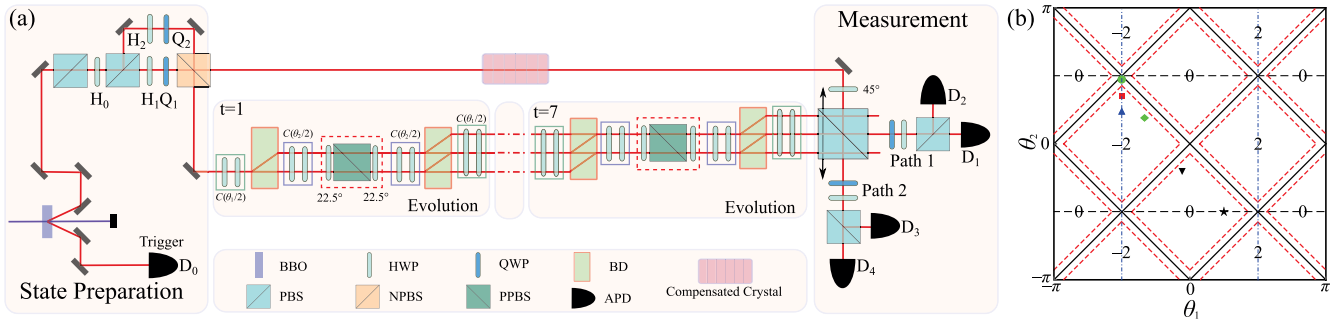

FIG. 1. (a) Experimental setup for the simulation of DQPTs using QWs. Pairs of single photons are generated via type-I spontaneous parametric down-conversion using a nonlinear β-barium-borate (BBO) crystal. One photon serves as a trigger and the other signal photon is prepared in an arbitrary linear polarization state using polarizing beam splitters (PBSs), half-wave plates (HWPs) and quarter-wave plates (QWPs) with certain setting angles, and a nonpolarizing beam splitter (NPBS). Coin rotations and conditional translations are realized by two HWPs and a beam displacer (BD), respectively. For nonunitary QWs, a sandwich-type HWP-PPBS-HWP setup is inserted to introduce the partial measurement, where PPBS is an acronym for a partially polarizing beam splitter. Avalanche photodiodes (APDs) detect the signal and heralding photons. (b) Phase diagram for QWs governed by Floquet operators U and $\tilde{U}$, labeled by the winding number ν as a function of coin parameters (θ_1, θ_2). Note that phase boundaries and winding numbers for unitary QW dynamics governed by U and nonunitary dynamics governed by $\tilde{U}$ are the same. Dashed red lines represent boundaries between $\mathcal{PT}$-symmetry-unbroken and broken regimes for $\tilde{U}$, with $\mathcal{PT}$-symmetry-broken regimes lying in between the red lines near topological phase boundaries, which are represented by solid black lines. The black star represents coin parameters of the initial Floquet operator U^i or $\tilde{U}^i$; other symbols indicate coin parameters of final Floquet operators in different cases.

inner products of the initial and time-evolved states of the single-photon dynamics via inference-based measurements, from which we construct quantities such as the rate function and DTOPs for the many-body dynamics. An advantage of photonic QW dynamics lies in the relative ease of introducing decoherence and loss, which further allows us to experimentally investigate DQPTs for mixed states and in nonunitary dynamics for the first time. Our experimental results agree well with theoretical predictions [28,29,40].

Simulating quench between topological phases.—We study DQPTs in quench dynamics using discrete-time QWs on a one-dimensional homogeneous lattice L ($L \in \mathbb{Z}$), where we use polarization states of single photons $\{|H\rangle, |V\rangle\}$ to represent coin states and spatial modes to encode walker states. As illustrated in Fig. 1(a), the main component of our setup is a cascaded interferometric network, where QW dynamics is governed by the Floquet operator

$$U = C(\theta_1/2)SC(\theta_2)SC(\theta_1/2). \tag{1}$$

Here, the coin operator $C(\theta)$ rotates the single-photon polarization by θ about the y axis. The shift operator S moves the walker in $|H\rangle$ ($|V\rangle$) to the left (right) by one lattice site.

Importantly, U can have nontrivial topological properties, as the corresponding effective Hamiltonian H_{eff} can have topologically nontrivial Floquet bands characterized by finite winding numbers [9,39,41]. Here H_{eff} is defined through $U = e^{-iH_{\text{eff}}}$. As illustrated in Fig. 1(b), winding numbers associated with these Floquet bands are tunable through the coin parameters (θ_1, θ_2).

For a typical QW process, the photon is initialized in a localized state $|\psi^i\rangle$ and is subject to repeated operations of U. At the tth step, the photon is in the state $|\psi(t)\rangle = U^t|\psi^i\rangle = e^{-iH_{\text{eff}}t}|\psi^i\rangle$. If we choose $|\psi^i\rangle$ to be an eigenstate of $U^i = e^{-iH^i_{\text{eff}}}$, the resulting QW dynamics is essentially a single-photon discrete-time quench process driven by the effective Hamiltonian H_{eff}. Because of the lattice-translational symmetry, dynamics in different quasimomentum k sectors are decoupled, which leads to a coherent superposition of time evolutions at different quasimomenta. This enables us to map the single-photon quench process into a quench between many-body Floquet topological phases associated with H^i_{eff} and H_{eff}, where time evolutions in different k sectors are also decoupled, but the many-body wave function is a direct product of single-particle states at different quasimomenta. Crucially, Floquet operators U^i with localized eigenstates exist, whose coin parameters are on the horizontal black dashed lines in Fig. 1(b). The corresponding H^i_{eff} are topologically trivial with $\nu^i = 0$. For contrast, in the following, we label the Floquet operator driving the QW as U^f, with ν^f the corresponding winding number. It is interesting to note that, whereas DQPTs do not actually occur in QWs of single photons, we are able to simulate DQPTs in quench dynamics of many-body topological systems using our setup.

Initialization and detection.—We initialize the walker photon at $x = 0$ (x is the site index), with its coin state given by the density matrix $\rho_0 = p|\psi^i_-\rangle\langle\psi^i_-| + (1-p)|\psi^i_+\rangle\langle\psi^i_+|$, where $|\psi^i_\pm\rangle = (|H\rangle \mp i|V\rangle)/\sqrt{2}$. The initial state is therefore

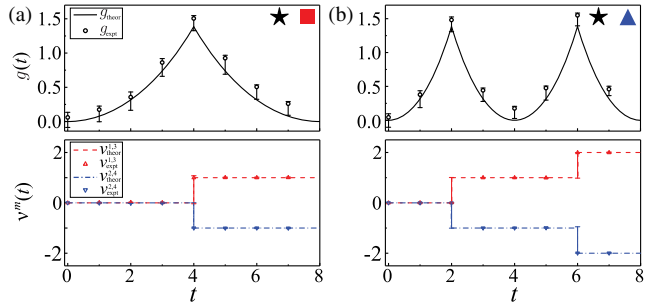

FIG. 2. Rate function (upper) and $\nu^m(t)$ (lower) of seven-step unitary QWs as functions of time steps. The initial state of the walker-coin system is $|x=0\rangle \otimes |\psi_-^i\rangle$. QWs are governed by U^f with (a) $(\theta_1^f = -\pi/2, \theta_2^f = 3\pi/8)$ and (b) U^f with $(\theta_1^f = -\pi/2, \theta_2^f = \pi/4)$, respectively. Error bars are derived from simulations where we consider all the systematic inaccuracies of the experiment. Asymmetry in error bars is due to decoherence.

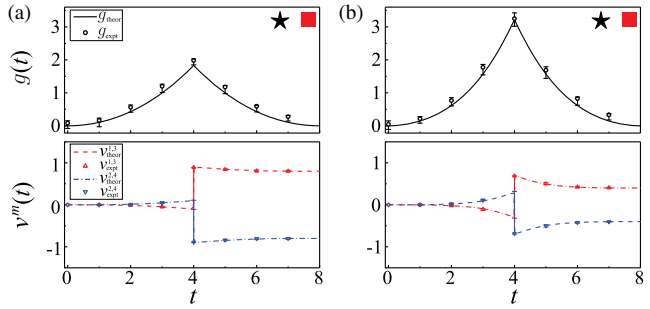

FIG. 3. Rate function (upper) and $\nu^m(t)$ (lower) of a seven-step unitary QW. The walker starts at $x = 0$ and the QW is governed by the final Floquet operator U^f with $(\theta_1^f = -\pi/2, \theta_2^f = 3\pi/8)$. The initial coin state is a mixed state with (a) $p = 0.9$ and (b) $p = 0.7$, respectively. Error bars are derived from simulations, where we consider all the systematic inaccuracies of the experiment.

a pure state when $p = \{0, 1\}$ and a mixed state otherwise. Importantly, $|x=0\rangle \otimes |\psi_\pm^i\rangle$ are eigenstates of U^i with the coin parameters $(\theta_1^i = \pi/4, \theta_2^i = -\pi/2)$. We then implement QWs governed by U^f with coin parameters (θ_1^f, θ_2^f). To facilitate measurement and reduce experimental error, for most of our experiments, we choose (θ_1^f, θ_2^f) on blue dash-dotted lines in Fig. 1(b), as the spatial spread of the resulting QW dynamics is small.

As the time evolution in each k sector is governed by U_k^f, the Fourier component of U^f, we construct the Loschmidt amplitude $G(k,t)$ from its Fourier component $\bar{P}(p,x,t)$ according to

$$G(k,t) \coloneqq \mathrm{Tr}[\rho_0 (U_k^f)^t] = \sum_x e^{-ikx} \bar{P}(p,x,t), \qquad (2)$$

where $\bar{P}(p,x,t) = p\langle\psi_-^i|\psi_-(x,t)\rangle + (1-p)\langle\psi_+^i|\psi_+(x,t)\rangle$, and $|\psi_\pm(x,t)\rangle = \sum_k e^{ikx}(U_k^f)^t|\psi_\pm^i\rangle$. Experimentally, $\bar{P}(p,x,t)$ is measured by performing interference-based measurements at the tth step [41,42].

We then construct the rate function according to $g(t) = -\sum_{k\in 1\mathrm{BZ}} \ln |G(k,t)|^2$. Note that by construction, $g(t)$ is the rate function of a quench between many-body Floquet topological phases of fermions, where the initial state is a direct product of single-particle density matrices ρ_0 at different quasimomenta in the first Brillouin zone (1BZ) and the corresponding many-body Loschmidt amplitude $G(t)$ is given by $G(t) = \prod_{k\in 1\mathrm{BZ}} G(k,t)$.

From the measured $G(k,t)$, we further calculate DTOPs characterizing DQPTs, which are defined as [27]

$$\nu^m(t) = \frac{1}{2\pi}\int_{k_m}^{k_{m+1}} \frac{\partial \phi_k^G(t)}{\partial k} dk, \qquad (3)$$

where the Pancharatnam geometric phase $\phi_k^G(t) = \phi_k(t) - \phi_k^{\mathrm{dyn}}(t)$. Here $\phi_k(t)$ is defined through $G(k,t) = |G(k,t)|e^{i\phi_k(t)}$, and $\phi_k^{\mathrm{dyn}}(t)$ is the dynamic phase (see Supplemental Material [41]). k_m $(m = 1, 2, \ldots)$ are fixed points of the dynamics, where the corresponding density matrices do not evolve in time and $\phi_k^G(t)$ vanishes at all times. $\nu^m(t)$ therefore characterizes the $S^1 \to S^1$ mapping from the momentum submanifold between k_m and k_{m+1} to $e^{i\phi_k^G(t)}$.

Physically, DTOPs measure the geometric phase accumulated by the time-evolved wave function and characterize different dynamic regimes separated by the DQPT [22]. Further, it can only change value at a topological DQPT with $G(k_c, t_c) = 0$, where the geometric phase becomes ill-defined. Here, k_c lies between adjacent fixed points and $t_c = (2n-1)t_0$ $(n \in \mathbb{N})$, with the critical timescale $t_0 = \pi/(2E_{k_c}^f)$ and $\pm E_k^f$ is the quasienergy of U_k^f (see Supplemental Material [41]). While topological DQPTs only occur for quenches between distinct topological phases, abrupt jumps in $\nu^m(t)$ can serve as signals for the dynamic characterization of equilibrium topological phases.

DQPT in unitary dynamics.—We first study DQPTs for pure states in unitary dynamics. We initialize photons in the coin state $|\psi_-^i\rangle$ at $x = 0$. The photons are then subject to unitary time evolutions governed by the Floquet operator U^f with $(\theta_1^f = -\pi/2, \theta_2^f = 3\pi/8)$, which simulates a quench between Floquet topological phases with $\nu^i = 0$ and $\nu^f = -2$. Here, the fixed points $k_{1,2,3,4} = \{-\pi, -\pi/2, 0, \pi/2\}$ and $k_c = \{\pm\pi/4, \pm 3\pi/4\}$. Note U_k^f has a discrete symmetry $U_k^f = U_{k+\pi}^f$ in addition to the time-reversal symmetry. Under these symmetries, $E_{k_c}^f$ are degenerate and there is only one critical timescale $t_0 = 4$. In Fig. 2(a), we show the rate function, which becomes nonanalytic at the first critical time $t_c = t_0$. Whereas it is difficult to directly identify nonanalyticities of $g(t)$ in discrete-time dynamics, the measured $g(t)$ peaks at critical times and DQPTs are unambiguously revealed by jumps

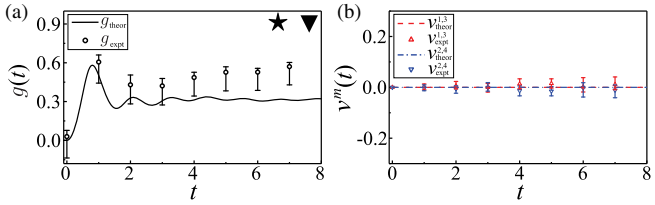

FIG. 4. (a) Rate function and (b) $\nu^m(t)$ of a seven-step unitary QW. The QW is governed by the final Floquet operator U^f with $(\theta_1^f = -\pi/16, \theta_2^f = -3\pi/16)$, which has the same winding number as that of the initial state. Error bars are derived from simulations, where we consider all the systematic inaccuracies of the experiment.

in the quantized DTOP across t_c. The critical times are further confirmed by particularly large error bars in the measured $\nu^m(t_c)$ (see Supplemental Material [41]), where small perturbations have significant impact on the DTOP. Because of the symmetry of U_k^f, we have $\nu^{1,3}(t) = -\nu^{2,4}(t)$, where $\nu^4(t)$ is integrated in the range $(\pi/2, \pi)$.

We then fix the initial coin state and change the final Floquet operator to U^f with $(\theta_1^f = -\pi/2, \theta_2^f = \pi/4)$. As shown in Fig. 2(b), the critical timescale changes to $t_0 = 2$, and the rate function becomes nonanalytic at odd multiples of t_0. The quantized DTOPs also feature abrupt jumps at critical times. As locations of k_m and k_c are the same as those of the previous case, there is only one critical timescale as well.

In the second case study, we initialize photons at $x = 0$ and in a mixed coin state characterized by ρ_0 with $p = 0.7$ and $p = 0.9$, respectively. The QW is governed by U^f with $(\theta_1^f = -\pi/2, \theta_2^f = 3\pi/8)$. Whereas the resulting QW dynamics still simulates quenches between topological phases with $\nu^i = 0$ and $\nu^f = -2$, coin states of time-evolved states remain mixed. As shown in Fig. 3, while the occurrence of DQPTs are still signaled by nonanalyticities in the rate functions, DTOPs are typically not quantized. This is because $\phi_k^G(t)$ do not vanish at k_m at all times, such that $e^{i\phi_k^G}$ no longer forms a closed S^1 manifold between k_m and k_{m+1}. Consequently, $\nu^m(t)$ is no longer the winding number characterizing such a map. These results are consistent with previous theoretical studies [28,29]. Note locations of k_m and k_c are the same as in the previous cases.

For comparison, we choose U^f with $(\theta_1^f = -\pi/16, \theta_2^f = -3\pi/16)$ and study the case where the quench dynamics is between phases with $\nu^i = 0$ and $\nu^f = 0$. As shown in Fig. 4, the rate function is smooth in time and $\nu^m(t)$ remains zero, indicating the absence of DQPTs. Here $k_m = \{0, \pm\pi/2, \pi\}$.

DQPT in nonunitary dynamics.—The ease of introducing loss in photonics further allows us to explore DQPTs in nonunitary dynamics [40,43]. We enforce nonunitary dynamics by performing a partial measurement $M_e = \mathbb{1}_w \otimes \sqrt{l}|-\rangle\langle -|$ in the basis $\{|\pm\rangle\}$ at each time step, with $\mathbb{1}_w = \sum_x |x\rangle\langle x|$, $|\pm\rangle = (|H\rangle \pm |V\rangle)/\sqrt{2}$ and l as the loss parameter, which is fixed at $l = 0.36$ in our experiment. The nonunitary QW is then governed by

$$\tilde{U} = \gamma C(\theta_1/2) SC(\theta_2/2) MC(\theta_2/2) SC(\theta_1/2), \quad (4)$$

where $M = \mathbb{1}_w \otimes (|+\rangle\langle +| + \sqrt{1-l}|-\rangle\langle -|)$ and $\gamma = (1-l)^{-1/4}$.

Topological properties of $\tilde{U}$ are characterized by winding numbers defined through the global Berry phase [44–46]. The resulting phase diagram is the same as that of U (see Supplemental Material [41]). Crucially, $\tilde{U}$ also possess parity-time ($\mathcal{PT}$) symmetry; therefore its quasienergy spectra can be entirely real in the $\mathcal{PT}$-symmetry-unbroken regime [47–49], in contrast to the regime with spontaneously broken $\mathcal{PT}$ symmetry. The boundary between regimes with unbroken and broken $\mathcal{PT}$ symmetry is plotted in Fig. 1(b) as red dashed lines, with $\mathcal{PT}$-symmetry-broken regimes surrounding topological phase boundaries. It can be shown that DQPTs necessarily occur for quench processes between distinct Floquet topological phases in the $\mathcal{PT}$-symmetry-unbroken regime [40,41].

Similar to the unitary case, we initialize photons in the state $|x = 0\rangle \otimes |\tilde{\psi}_-^i\rangle$, with the corresponding $\tilde{U}^i$ in the

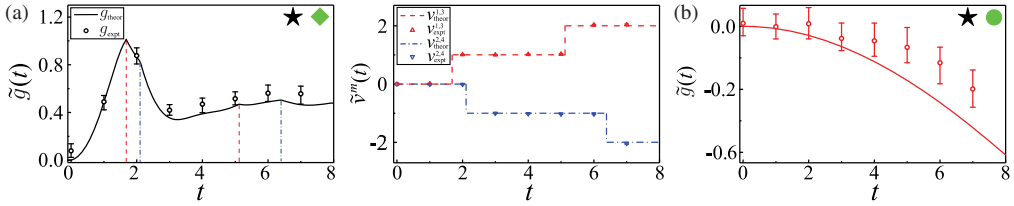

FIG. 5. (a) Rate function and $\tilde{\nu}^m(t)$ of a seven-step nonunitary QW with a loss parameter $l = 0.36$. The initial state of the walker-coin system is $|0\rangle \otimes |\tilde{\psi}_-^i\rangle$. The QW is governed by the nonunitary Floquet operator $\tilde{U}^f$ with $(\theta_1^f = -\pi/3, \theta_2^f = \pi/5)$. (b) Rate function of the QW governed by $\tilde{U}^f$ with $[\theta_1^f = -\pi/2, \theta_2^f = (\pi - \xi)/2]$, where $\xi = \arccos(1/\alpha)$ and $\alpha = (1 + \sqrt{1-l})/(2\sqrt[4]{1-l})$. The two critical timescales are $t_0 = \{1.7183, 2.1482\}$, which give rise to nonanalyticities in the rate function as indicated by vertical dashed lines in (a). Theoretically calculated fixed points are located at $k_{1,2,3,4} = \{-1.0094\pi, -0.4470\pi, -0.0094\pi, 0.5530\pi\}$ and the critical momenta $k_c = \{-0.7888\pi, -0.1534\pi, 0.2112\pi, 0.8466\pi\}$. Experimental errors are due to photon-counting statistics.

$\mathcal{PT}$-symmetry-unbroken regime with $\nu^i = 0$ and $|x = 0\rangle \otimes |\tilde{\psi}^i_-\rangle$ as the ground state of $\tilde{U}^i$. The walker is evolved under the final nonunitary Floquet operator $\tilde{U}^f$ with $(\theta^f_1 = -\pi/3, \theta^f_2 = \pi/5)$, which is in the $\mathcal{PT}$-symmetry-unbroken regime with $\nu^f = -2$. The Loschmidt amplitude, the rate function $\tilde{g}(t)$, and the DTOP $\tilde{\nu}^m(t)$ for nonunitary dynamics can be constructed similar to the unitary case (see Supplemental Material [41]). As illustrated in Fig. 5(a), nonanalyticities in the rate function have two distinct timescales, which correspond to two different DTOPs [see Fig. 5(b)], both quantized and demonstrating abrupt jumps at odd multiples of the corresponding critical timescale.

The emergence of two critical timescales is due to the breaking of time-reversal symmetry of the nonunitary dynamics [40]. In this case, whereas fixed points still exist when U^i and U^f are in the $\mathcal{PT}$-symmetry-unbroken regime and have different winding numbers, they are no longer located at high-symmetry points (see Supplemental Material [41]). As a consequence, $\nu^{1,3}(t)$ and $\nu^{2,4}(t)$ feature jumps with distinct critical timescales, characterized by critical momenta with different quasienergies.

Finally, we study the case when the final nonunitary Floquet operator is in the $\mathcal{PT}$-symmetry-broken regime. The resulting rate function is shown in Fig. 5(b), where no DQPTs can be identified. As fixed points are also absent in the dynamics, DTOPs cannot be defined in this case [40].

Final remarks.—We have showcased photonic QWs as a powerful platform for the simulation of DQPTs in quench dynamics of many-body topological systems. A key requirement for our simulation scheme is the coherence between different Fourier components of the wave function, which, for a single-photon QW, is guaranteed by the quantum superposition of wave function amplitudes at different quasimomenta. Our experiment opens up the avenue of investigating DQPTs and related dynamic topological phenomena using QW dynamics, whose flexible control paves the way for future studies in novel contexts such as engineered nonunitary dynamics, with decoherence, or in higher dimensions.

This work has been supported by the Natural Science Foundation of China (Grants No. 11474049, No. 11674056, and No. 11522545) and the Natural Science Foundation of Jiangsu Province (Grant No. BK20160024). W. Y. acknowledges support from the National Key R&D Program (Grants No. 2016YFA0301700 and No. 2017YFA0304100).

K. W. and X. Q. contributed equally to this work.

*wyiz@ustc.edu.cn
†gnep.eux@gmail.com

[1] L. D. Landau, On the theory of phase transitions, Phys. Z. Sowjetunion **11**, 26 (1937).
[2] M. Z. Hasan and C. L. Kane, Colloquium: Topological insulators, Rev. Mod. Phys. **82**, 3045 (2010).
[3] X. L. Qi and S. C. Zhang, Topological insulators and superconductors, Rev. Mod. Phys. **83**, 1057 (2011).
[4] G. Jotzu, M. Messer, R. Desbuquois, M. Lebrat, T. Uehlinger, D. Greif, and T. Esslinger, Experimental realization of the topological Haldane model with ultracold fermions, Nature (London) **515**, 237 (2014).
[5] N. Fläschner, B. S. Rem, M. Tarnowski, D. Vogel, D.-S. Lühmann, K. Sengstock, and C. Weitenberg, Experimental reconstruction of the Berry curvature in a Floquet Bloch band, Science **352**, 1091 (2016).
[6] B. Song, L. Zhang, C. He, T. F. J. Poon, E. Hajiyev, S. Zhang, X.-J. Liu, and G.-B. Jo, Observation of symmetry-protected topological phases with ultracold fermions, Sci. Adv. **4**, eaao4748 (2018).
[7] M. Tarnowski, F. Nur-Unal, N. Flaschner, B. S. Rem, A. Eckard, K. Sengstock, and C. Weitenberg, Characterizing topology by dynamics: Chern number from linking number, arXiv:1709.01046.
[8] N. Fläschner, D. Vogel, M. Tarnowski, B. S. Rem, D.-S. Lühmann, M. Heyl, J. C. Budich, L. Mathey, K. Sengstock, and C. Weitenberg, Observation of dynamical vortices after quenches in a system with topology, Nat. Phys. **14**, 265 (2018).
[9] T. Kitagawa, M. A. Broome, A. Fedrizzi, M. S. Rudner, E. Berg, I. Kassal, A. Aspuru-Guzik, E. Demler, and A. G. White, Observation of topologically protected bound states in photonic quantum walks, Nat. Commun. **3**, 882 (2012).
[10] F. Cardano, M. Maffei, F. Massa, B. Piccirillo, C. de Lisio, G. D. Filippis, V. Cataudella, E. Santamato, and L. Marrucci, Statistical moments of quantum-walk dynamics reveal topological quantum transitions, Nat. Commun. **7**, 11439 (2016).
[11] F. Cardano, A. D'Errico, A. Dauphin, M. Maffei, B. Piccirillo, C. de Lisio, G. D. Filippis, V. Cataudella, E. Santamato, L. Marrucci, M. Lewenstein, and P. Massignan, Detection of Zak phases and topological invariants in a chiral quantum walk of twisted photons, Nat. Commun. **8**, 15516 (2017).
[12] L. Xiao, X. Zhan, Z. H. Bian, K. K. Wang, X. Zhang, X. P. Wang, J. Li, K. Mochizuki, D. Kim, N. Kawakami, W. Yi, H. Obuse, B. C. Sanders, and P. Xue, Observation of topological edge states in parity-time-symmetric quantum walks, Nat. Phys. **13**, 1117 (2017).
[13] J. M. Zeuner, M. C. Rechtsman, Y. Plotnik, Y. Lumer, S. Nolte, M. S. Rudner, M. Segev, and A. Szameit, Observation of a Topological Transition in the Bulk of a Non-Hermitian System, Phys. Rev. Lett. **115**, 040402 (2015).
[14] X. Zhan, L. Xiao, Z. Bian, K. Wang, X. Qiu, B. C. Sanders, W. Yi, and P. Xue, Detecting Topological Invariants in Nonunitary Discrete-Time Quantum Walks, Phys. Rev. Lett. **119**, 130501 (2017).
[15] P. Jurcevic, H. Shen, P. Hauke, C. Maier, T. Brydges, C. Hempel, B. P. Lanyon, M. Heyl, R. Blatt, and C. F. Roos, Direct Observation of Dynamical Quantum Phase Transitions in an Interacting Many-Body System, Phys. Rev. Lett. **119**, 080501 (2017).
[16] J. Zhang, G. Pagano, P. W. Hess, A. Kyprianidis, P. Becker, H. Kaplan, A. V. Gorshkov, Z.-X. Gong, and C. Monroe, Observation of a many-body dynamical phase transition

with a 53-qubit quantum simulator, Nature (London) **551**, 601 (2017).
[17] X.-Y. Guo, C. Yang, Y. Zeng, Y. Peng, H.-K. Li, H. Deng, Y.-R. Jin, S. Chen, D. Zheng, and H. Fan, Observation of dynamical quantum phase transition by a superconducting qubit simulation, arXiv:1806.09269.
[18] H. Bernie, S. Schwartz, A. Keesling, H. Levine, A. Omran, H. Pichler, S. Choi, A. Zibrov, M. Endres, M. Greiner, V. Vuletić, and M. D. Lukin, Probing many-body dynamics on a 51-atom quantum simulator, Nature (London) **551**, 579 (2017).
[19] X. P. Wang, L. Xiao, X. Z. Qiu, K. K. Wang, W. Yi, and P. Xue, Detecting topological invariants and revealing topological phase transitions in discrete-time photonic quantum walks, Phys. Rev. A **98**, 013835 (2018).
[20] M. Heyl, A. Polkovnikov, and S. Kehrein, Dynamical Quantum Phase Transitions in the Transverse-Field Ising Mode, Phys. Rev. Lett. **110**, 135704 (2013).
[21] M. Heyl, Scaling and Universality at Dynamical Quantum Phase Transitions, Phys. Rev. Lett. **115**, 140602 (2015).
[22] M. Heyl, Dynamical quantum phase transitions: A review, Rep. Prog. Phys. **81**, 054001 (2018).
[23] M. E. Fisher, *The Nature of Critical Points, Lectures in Theoretical Physics* (University of Colorado Press, Boulder, Colorado, 1965), Vol. 7.
[24] C. N. Yang and T. D. Lee, Statistical theory of equations of state and phase transitions. I. Lattice gas and Ising model, Phys. Rev. **87**, 404 (1952).
[25] C. N. Yang and T. D. Lee, Statistical theory of equations of state and phase transitions. II. Lattice gas and Ising model, Phys. Rev. A **87**, 410 (1952).
[26] K. Brandner, V. F. Maisi, J. P. Pekola, J. P. Garrahan, and C. Flindt, Experimental Determination of Dynamical Lee-Yang Zeros, Phys. Rev. Lett. **118**, 180601 (2017).
[27] J. C. Budich and M. Heyl, Dynamical topological order parameters far from equilibrium, Phys. Rev. B **93**, 085416 (2016).
[28] U. Bhattacharya, S. Bandyopadhyay, and A. Dutta, Mixed state dynamical quantum phase transitions, Phys. Rev. B **96**, 180303 (2017).
[29] M. Heyl and J. C. Budich, Dynamical topological quantum phase transitions for mixed states, Phys. Rev. B **96**, 180304 (2017).
[30] U. Bhattacharya and A. Dutta, Emergent topology and dynamical quantum phase transitions in two-dimensional closed quantum systems, Phys. Rev. B **96**, 014302 (2017).
[31] X. Qiu, T.-S. Deng, G.-C. Guo, and W. Yi, Dynamical topological invariants and reduced rate functions for dynamical quantum phase transitions in two dimensions, Phys. Rev. A **98**, 021601(R) (2018).
[32] S. Vajna and B. Dora, Topological classification of dynamical phase transitions, Phys. Rev. B **91**, 155127 (2015).
[33] Z. Huang and A. V. Balatsky, Dynamical Quantum Phase Transitions: Role of Topological Nodes in Wave Function Overlaps, Phys. Rev. Lett. **117**, 086802 (2016).
[34] U. Bhattacharya and A. Dutta, Interconnections between equilibrium topology and dynamical quantum phase transitions in a linearly ramped Haldane model, Phys. Rev. B **95**, 184307 (2017).
[35] F. Zähringer, G. Kirchmair, R. Gerritsma, E. Solano, R. Blatt, and C. F. Roos, Realization of a Quantum Walk with One and Two Trapped Ions, Phys. Rev. Lett. **104**, 100503 (2010).
[36] A. Schreiber, K. N. Cassemiro, V. Potoček, A. Gábris, I. Jex, and Ch. Silberhorn, Decoherence and Disorder in Quantum Walks: From Ballistic Spread to Localization, Phys. Rev. Lett. **106**, 180403 (2011).
[37] M. Genske, W. Alt, A. Steffen, A. H. Werner, R. F. Werner, D. Meschede, and A. Alberti, Electric Quantum Walks with Individual Atoms, Phys. Rev. Lett. **110**, 190601 (2013).
[38] T. Nitsche, S. Barkhofen, R. Kruse, L. Sansoni, M. Štefaňák, A. Gábris, V. Potoček, T. Kiss, I. Jex, and Ch. Silberhorn, Probing measurement-induced effects in quantum walks via recurrence, Sci. Adv. **4**, eaar6444 (2018).
[39] T. Kitagawa, M. S. Rudner, E. Berg, and E. Demler, Exploring topological phases with quantum walks, Phys. Rev. A **82**, 033429 (2010).
[40] X. Qiu, T.-S. Deng, Y. Hu, P. Xue, and W. Yi, Fixed points and emergent topological phenomena in a parity-time-symmetric quantum quench, arXiv:1806.10268.
[41] See Supplemental Material at http://link.aps.org/supplemental/10.1103/PhysRevLett.122.020501 for details on experimental implementation, detection scheme, error analysis, as well as theoretical characterization of topological invariants and DQPTs.
[42] N. Y. Halpern, Jarzynski-like equality for the out-of-time-ordered correlator, Phys. Rev. A **95**, 012120 (2017).
[43] L. Zhou, Q. H. Wang, H. Wang, and J. Gong, Dynamical quantum phase transitions in non-Hermitian lattices, Phys. Rev. A **98**, 022129 (2018).
[44] J. Garrison and E. Wright, Complex geometrical phases for dissipative systems, Phys. Lett. A **128**, 177 (1988).
[45] S.-D. Liang and G.-Y. Huang, Topological invariance and global Berry phase in non-Hermitian systems, Phys. Rev. A **87**, 012118 (2013).
[46] S. Lieu, Topological phases in the non-Hermitian Su-Schieffer-Heeger model, Phys. Rev. B **97**, 045106 (2018).
[47] C. M. Bender and S. Boettcher, Real Spectra in Non-Hermitian Hamiltonians Having PT Symmetry, Phys. Rev. Lett. **80**, 5243 (1998).
[48] C. M. Bender, D. C. Brody, and H. F. Jones, Complex Extension of Quantum Mechanics, Phys. Rev. Lett. **89**, 270401 (2002).
[49] C. M. Bender, Making sense of non-Hermitian Hamiltonians, Rep. Prog. Phys. **70**, 947 (2007).